Supporting Information

Construction of novel Ag(0)-containing silver nanoclusters by regulating auxiliary phosphine ligands

Qing-Qing Ma,[a] Xue-Jing Zhai,[a] Jia-Hong Huang,[a] Yubing Si,[a] Xi-Yan Dong,[*a,b] Shuang-Quan Zang,[*a] and Thomas C. W. Mak[a,c]

[a]College of Chemistry, Zhengzhou University, Zhengzhou 450001, China.
[b]College of Chemistry and Chemical Engineering, Henan Polytechnic University, Jiaozuo 454000, China.
[c]Department of Chemistry, The Chinese University of Hong Kong, Shatin, New Territories, Hong Kong, SAR. China.

Email: dongxiyan0720@hpu.edu.cn; zangsqzg@zzu.edu.cn

Crystallographic data collection and structural refinement: SCXRD measurements of **Ag_{17}** and **Ag_{32}** were performed on a Rigaku XtaLAB Pro diffractometer with Mo-Kα (λ = 0.71073 Å) and Cu-Kα radiation (λ =1.5418 Å) at 200 K. Data collection and reduction were performed using the program CrysAlisPro.[1] The structure was solved with direct methods (*SHELXS*)[2] and refined by full-matrix least squares on F^2 using *OLEX2*,[3] which utilizes the *SHELXL2015* module.[4] All nonhydrogen atoms were anisotropically refined. Hydrogen atoms were placed in calculated positions refined using idealized geometries and assigned fixed isotropic displacement parameters. Detailed information about the X-ray crystal data, intensity collection procedure and refinement results for **Ag_{17}** and **Ag_{32}** compounds are summarized in Tables S1-S2. Partial bond lengths for **Ag_{17}** and **Ag_{32}** are summarized in Tables S3-S4.

Calculations Details： The calculations were performed using the semiempirical quantum mechanical methods GFN1-xTB packages.[5-7] The single crystal structure was chose as initial guess for ground state optimization at tight level. The optimized structure of the clusters preserved the basic characteristics of the input structure, only with slightly change in the bond length, bond angles and dihedral angles, which confirming the feasibility of GFN1-xTB methods for cluster calculations. The UV-Vis spectra were calculated by sTDA.[8,9]

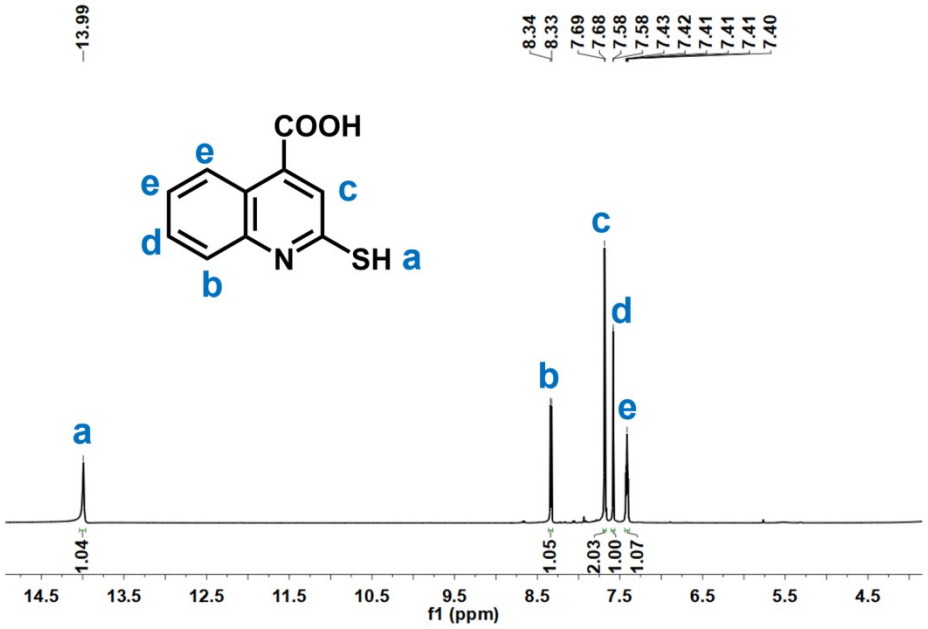

Figure S1. ^{1}H NMR (DMSO-d6) spectrum of quinoline-2-thiol (deprotonation)-4-carboxyl ligand.

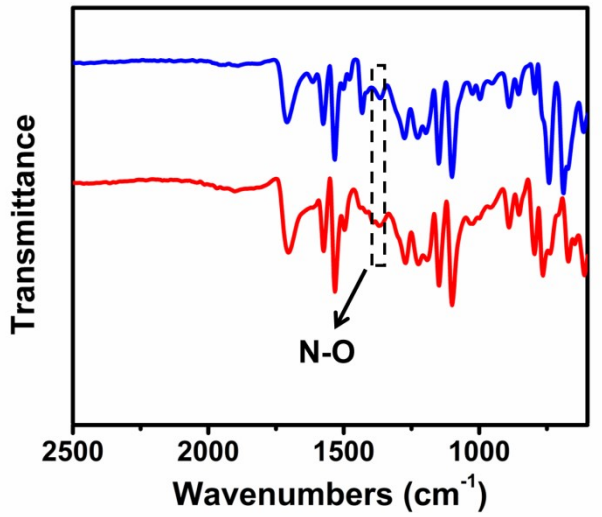

Figure S2. FT-IR spectra of $\mathbf{Ag_{17}}$ (blue line) and $\mathbf{Ag_{32}}$ (red line).

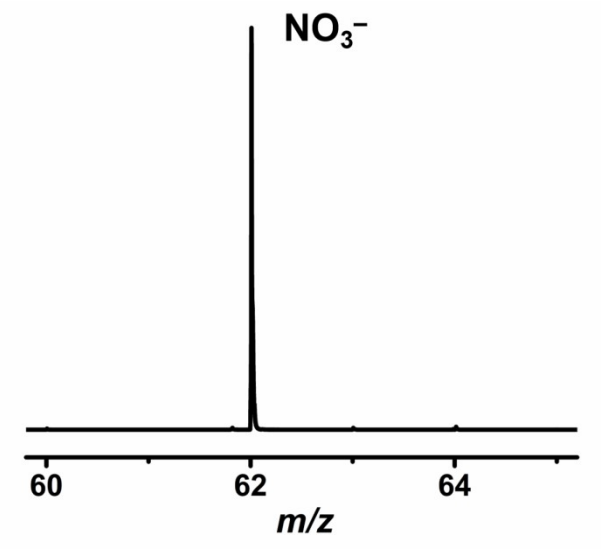

Figure S3. Mass spectrum of $\mathbf{Ag_{17}}$ and $\mathbf{Ag_{32}}$ in negative-ion mode confirming the presence of NO_3^-.

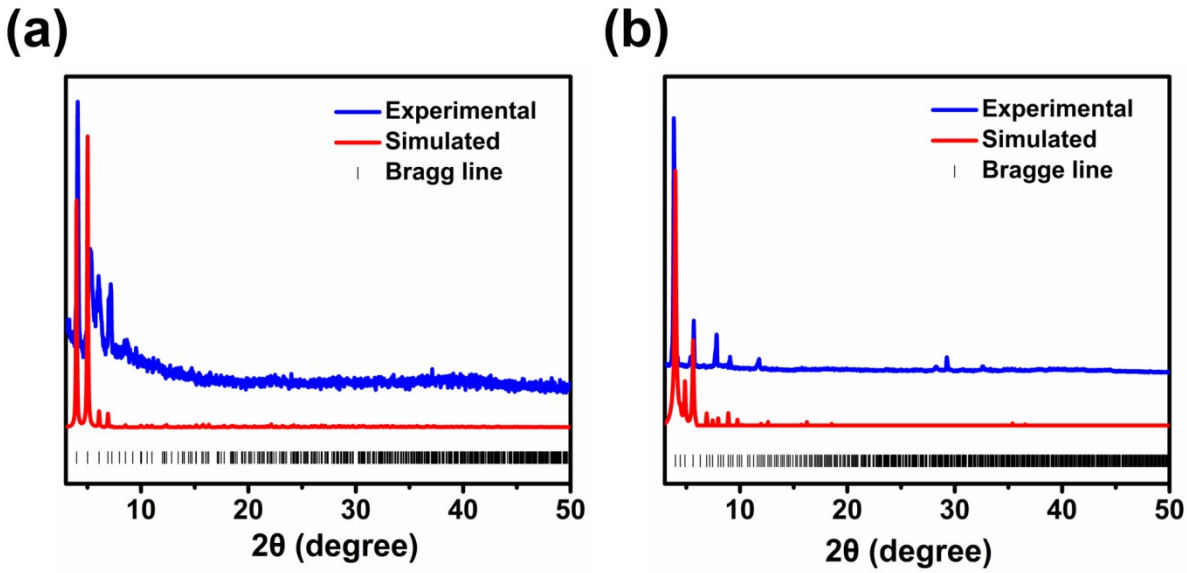

Figure S4. The simulated and experimental PXRD patterns of $\mathbf{Ag_{17}}$ (a) and $\mathbf{Ag_{32}}$ (b) crystals.

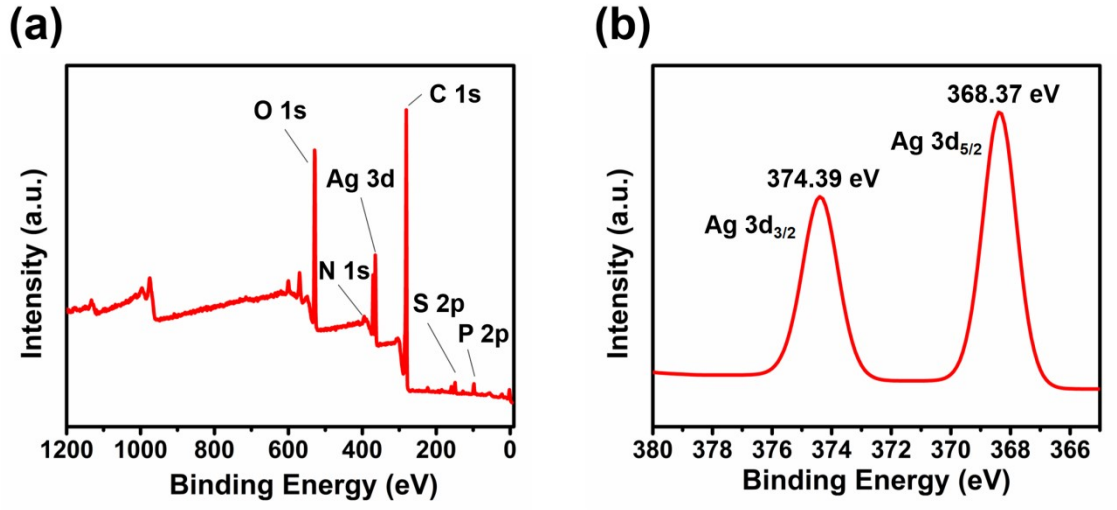

Figure S5. (a) XPS survey spectrum of **Ag_{17}**, confirming the presence of Ag, C, N, P, S, and O. (b) The expanded XPS spectrum in the Ag 3d region of **Ag_{17}**. In the Ag 3d spectrum, the Ag $3d_{5/2}$ peak (368.37 eV) is similar to those in other silver nanoparticles, indicating the existence of Ag^0 in **Ag_{17}**.

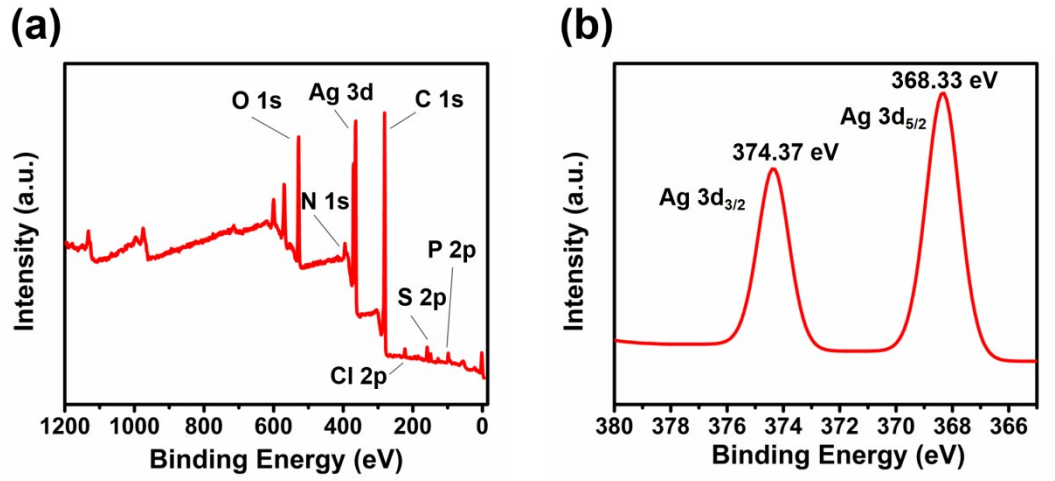

Figure S6. (a) XPS survey spectrum of **Ag_{32}**, confirming the presence of Ag, C, N, P, S, Cl, and O. (b) The expanded XPS spectrum in the Ag 3d region of **Ag_{32}**. In the Ag 3d spectrum, the Ag $3d_{5/2}$ peak (368.33 eV) is similar to those in other silver nanoparticles, indicating the existence of Ag^0 in **Ag_{32}**.

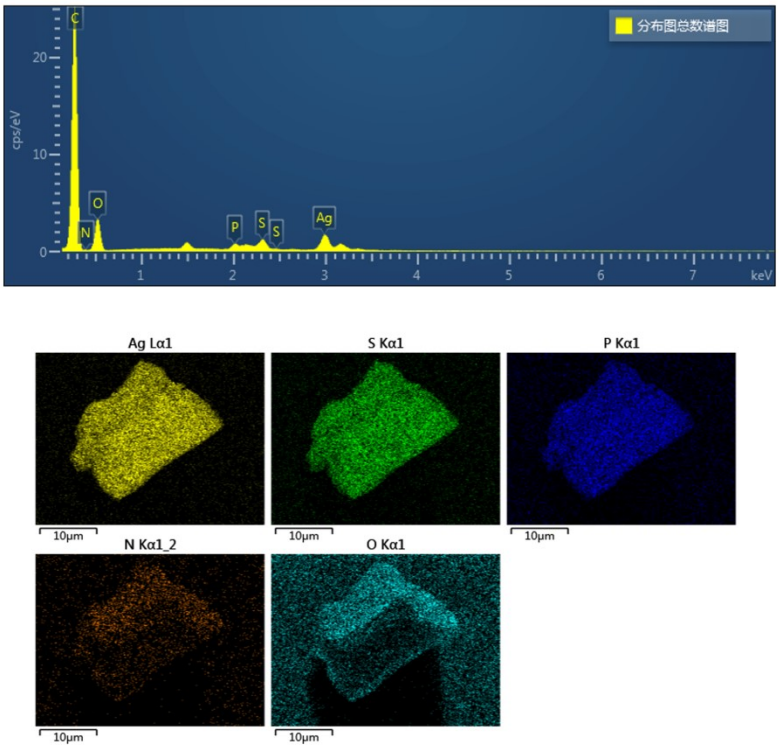

Figure S7. Morphologies of single crystals and energy dispersive spectroscopy (EDS) mapping results of $\mathbf{Ag_{17}}$.

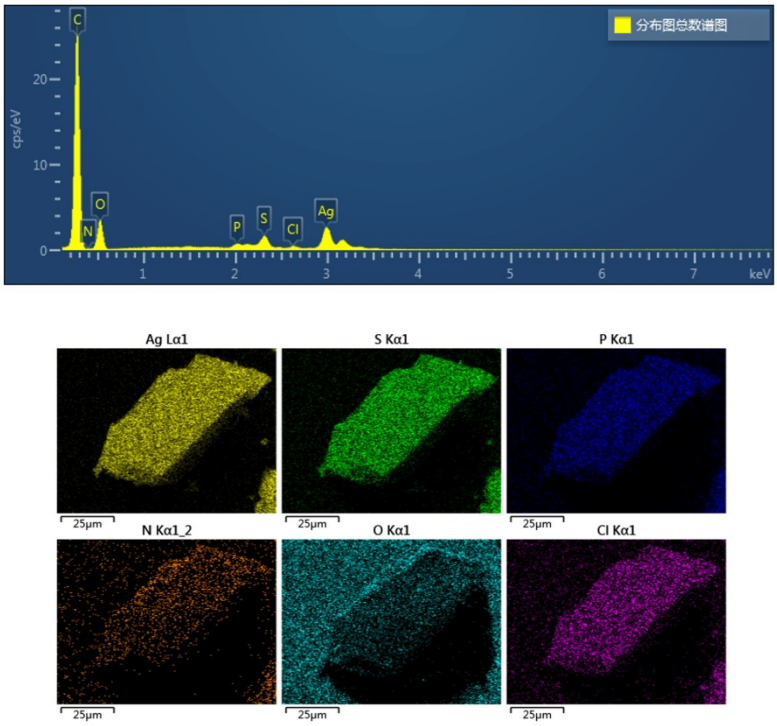

Figure S8. Morphologies of single crystals and energy dispersive spectroscopy (EDS) mapping results of $\mathbf{Ag_{32}}$.

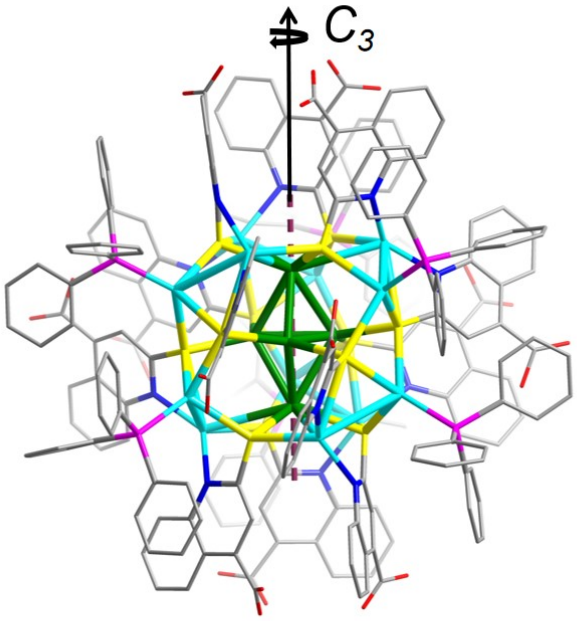

Figure S9. The structure of **Ag_{17}** with one C_3 axis. Atom colors: Ag, dark green and turquoise; S, yellow; P, purple; N, blue; C, gray; O, red.

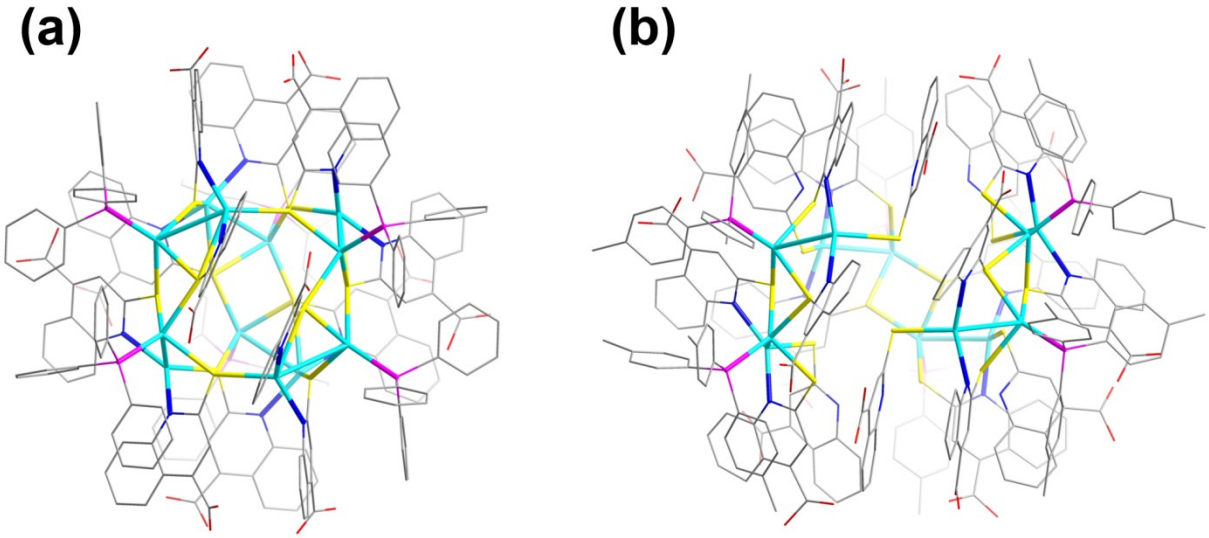

Figure S10. (a) The $Ag_{12}(L)_{12}(PPh_3)_6$ shell of **Ag_{17}**. (b) The $Ag_{12}(L)_{18}((P(Ph\text{-}^{p}CH_3)_3)_6$ shell of **Ag_{32}**. Atom colors: Ag, turquoise; S, yellow; P, purple; N, blue; C, gray; O, red.

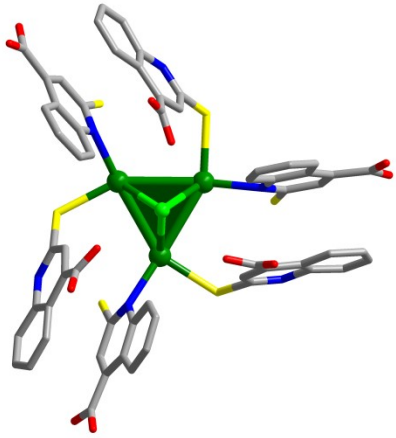

Figure S11. Ag_3-Cl triangular face of **Ag_{32}**. Atom colors: Ag, dark green; S, yellow; Cl, light green; N, blue; C, gray.

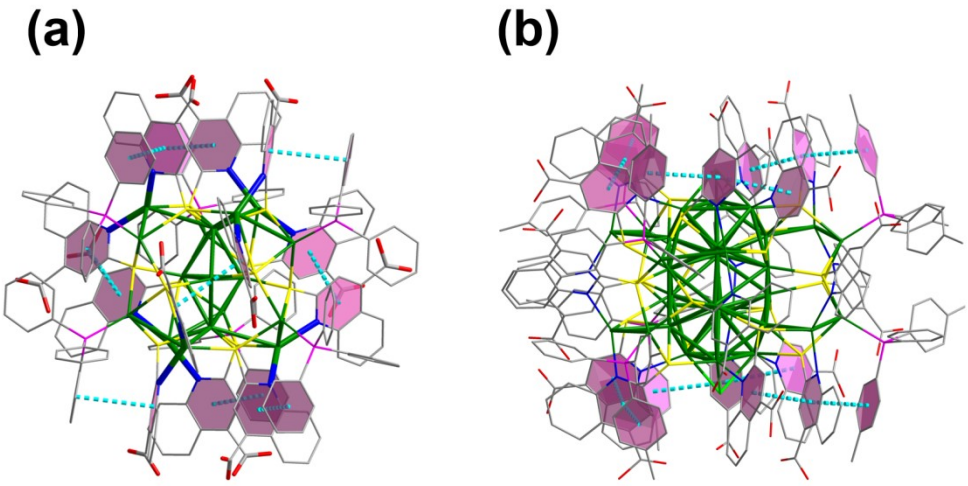

Figure S12. The π···π interactions of **Ag_{17}** (a) and **Ag_{32}** (b).

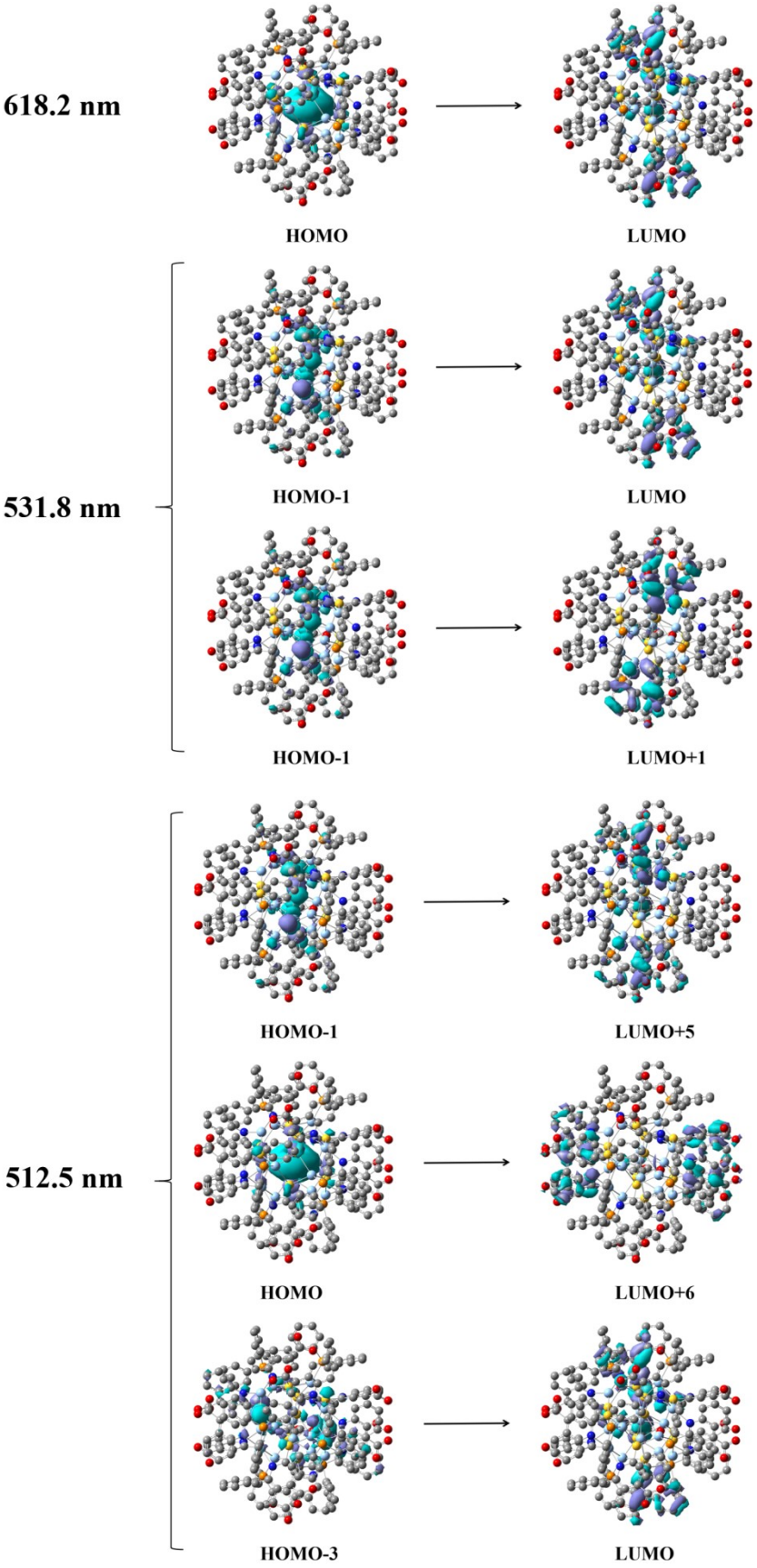
618.2 nm
HOMO
LUMO
531.8 nm
HOMO-1
LUMO
HOMO-1
LUMO+1
512.5 nm
HOMO-1
LUMO+5
HOMO
LUMO+6
HOMO-3
LUMO

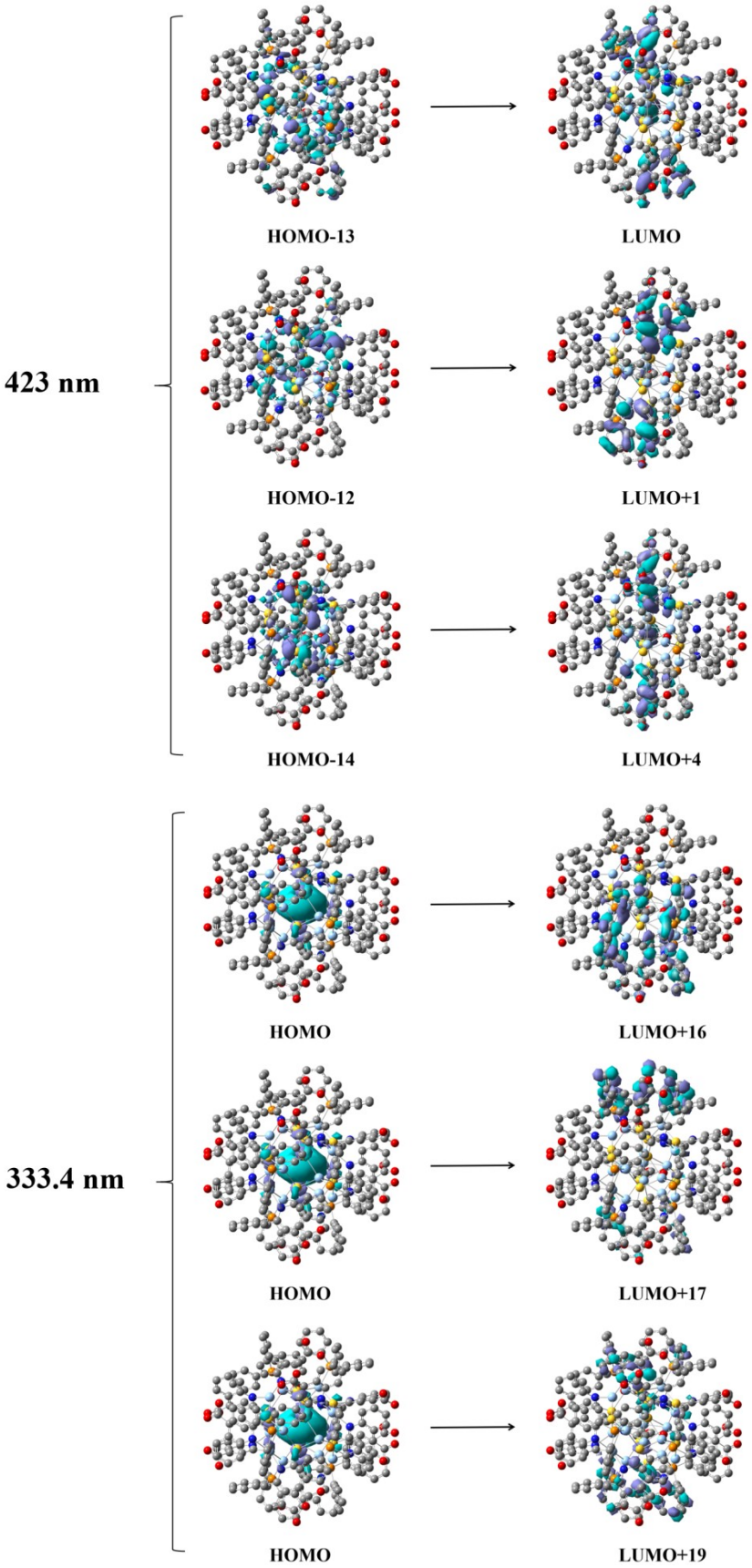

Figure S13. Transition-involved molecular orbitals of Ag_{17}.

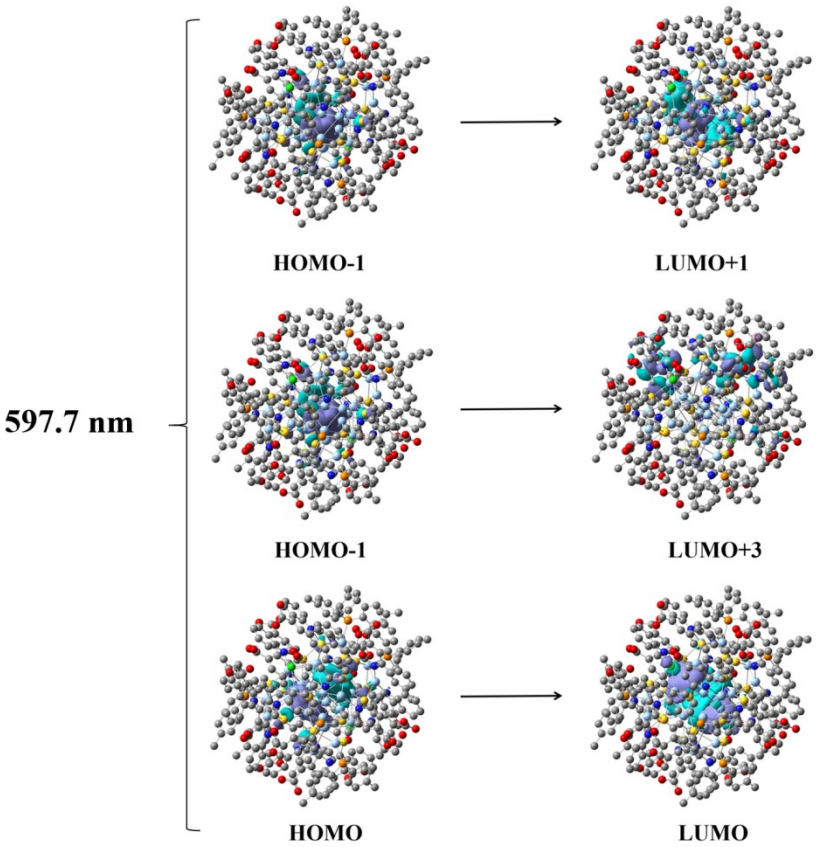
597.7 nm
HOMO-1
LUMO+1
HOMO-1
LUMO+3
HOMO
LUMO
451.0 nm
HOMO-11
LUMO+6
HOMO-13
LUMO+5
HOMO-19
LUMO+4

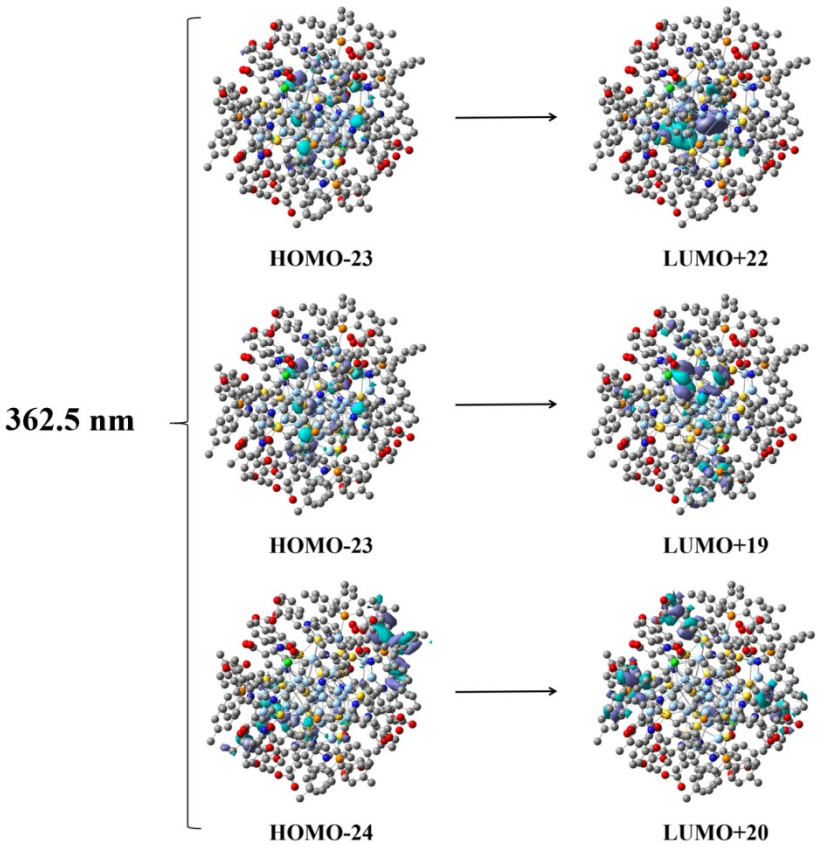

Figure S14. Transition-involved molecular orbitals of $\mathbf{Ag_{32}}$.

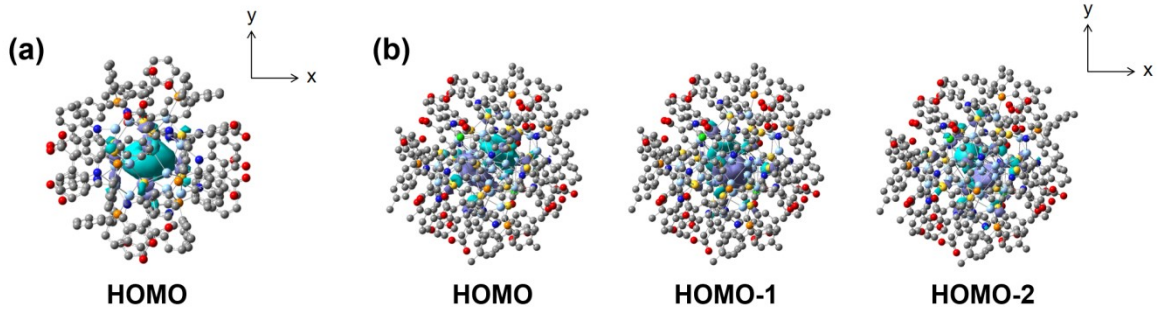

Figure S15. HOMOs of $\mathbf{Ag_{17}}$ (a) and $\mathbf{Ag_{32}}$ (b).

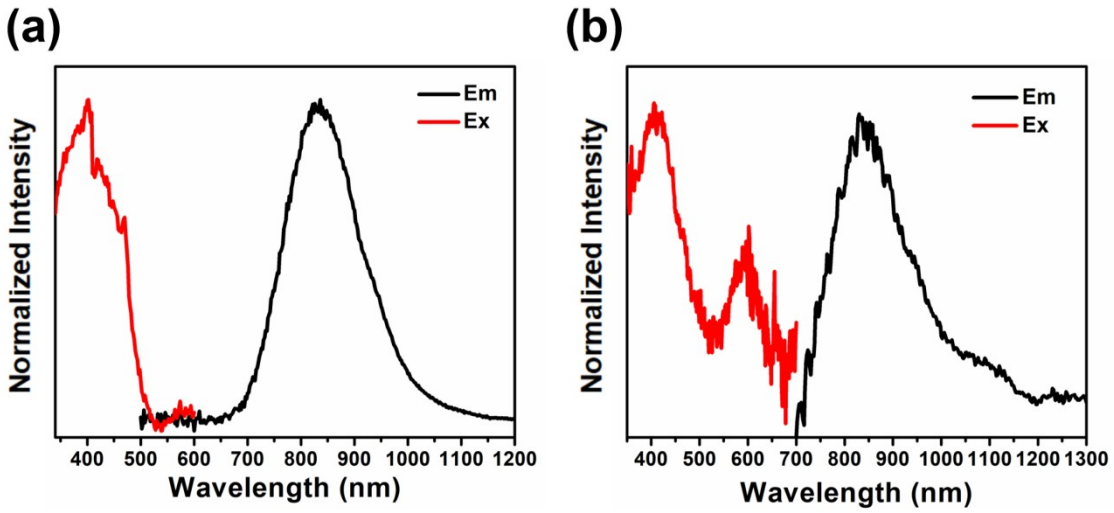

Figure S16. Luminescence excitation (red lines) and emission (black lines) spectra of $\mathbf{Ag_{17}}$ (a) and $\mathbf{Ag_{32}}$ (b) in CH_3OH solution.

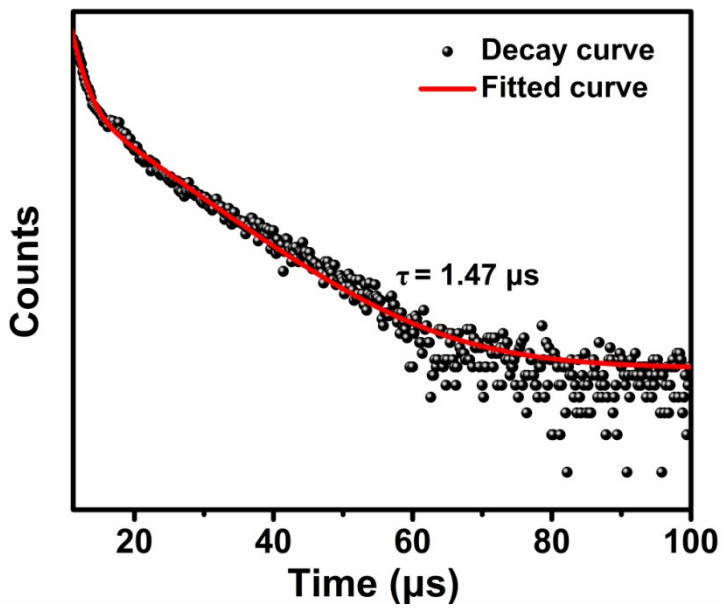

Figure S17. Temperature-dependent fluorescence decays of $\mathbf{Ag_{17}}$ in CH_3OH solution.

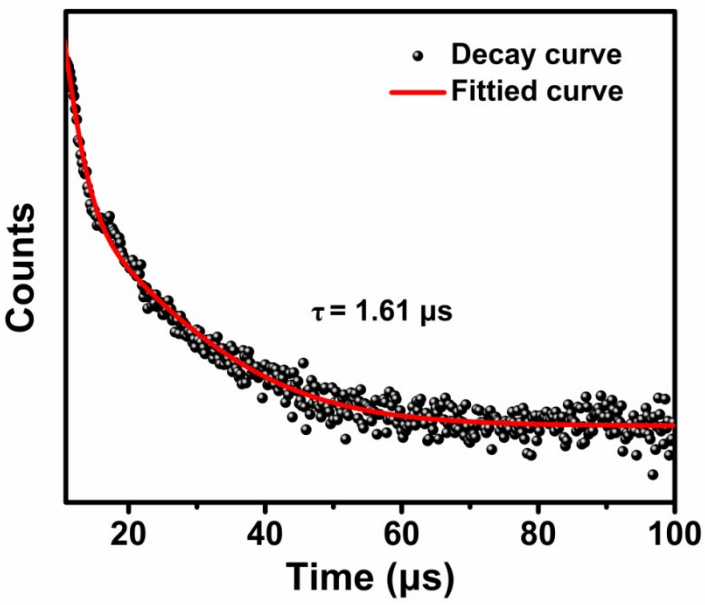

Figure S18. Temperature-dependent fluorescence decays of $\mathbf{Ag_{32}}$ in CH_3OH solution.

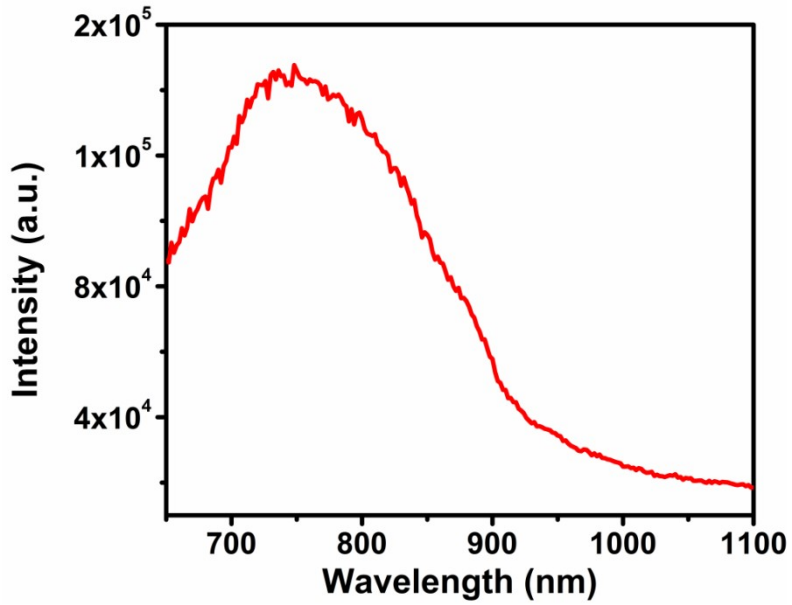

Figure S19. Emission spectra of $\mathbf{Ag_{17}}$ in solid state (excited at 400 nm).

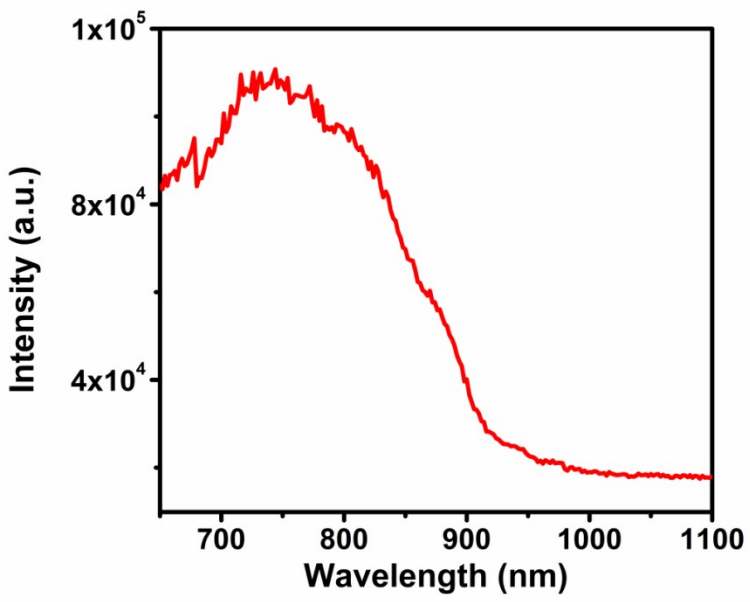

Figure S20. Emission spectra of $\mathbf{Ag_{32}}$ in solid state (excited at 400 nm).

Table S1. Crystallographic data and structure refinement for **Ag_{17}**.

CCDC number	2327808
Empirical formula	$C_{228}H_{162}Ag_{17}N_{12}O_{24}P_6S_{12}$
Formula weight	5857.90
Temperature/K	200.00
Crystal system	trigonal
Space group	*P*-31c
a/Å	25.5211(11)
b/Å	25.5211(11)
c/Å	28.9972(9)
α/°	90
β/°	90
γ/°	120
Volume/Å^3	16356.3(15)
Z	2
ρ_{calc}g/cm^3	1.189
μ/mm^{-1}	1.143
F(000)	5774.0
Crystal size/mm^3	0.15 × 0.12 × 0.1
Radiation	Mo Kα (λ = 0.71073)
2θ range for data collection/°	3.686 to 57.702
Index ranges	-34 ≤ h ≤ 26, -24 ≤ k ≤ 33, -37 ≤ l ≤ 37
Reflections collected	74038
Independent reflections	13090 [R_{int} = 0.0667, R_{sigma} = 0.0682]
Data/restraints/parameters	13090/453/560
Goodness-of-fit on F^2	1.025
Final R indexes [I>=2σ (I)]	R_1 = 0.1255, wR_2 = 0.3049
Final R indexes [all data]	R_1 = 0.1987, wR_2 = 0.3799
Largest diff. peak/hole/eÅ^{-3}	1.72/-1.34

$R_1 = \sum ||F_o|-|F_c|| / \sum |F_o|$. $wR_2 = [\sum w(F_o^2-F_c^2)^2 / \sum w(F_o^2)^2]^{1/2}$

Table S2. Crystallographic data and structure refinement for **Ag_{32}**.

CCDC number	2327952
Empirical formula	$C_{306}H_{234}Ag_{32}Cl_2N_{18}O_{36}P_6S_{18}$
Formula weight	9024.83
Temperature/K	200
Crystal system	cubic
Space group	*P*-43n
a/Å	44.3413(3)
b/Å	44.3413(3)
c/Å	44.3413(3)
α/°	90
β/°	90
γ/°	90
Volume/Å^3	87181.5(18)
Z	8
ρ_{calc}g/cm^3	1.375
μ/mm^{-1}	12.749
F(000)	35200.0
Crystal size/mm^3	0.48 × 0.45 × 0.36
Radiation	Cu Kα (λ = 1.54184)
2θ range for data collection/°	6.304 to 147.812
Index ranges	-50 ≤ h ≤ 39, -52 ≤ k ≤ 37, -55 ≤ l ≤ 15
Reflections collected	96491
Independent reflections	24931 [R_{int} = 0.0886, R_{sigma} = 0.0823]
Data/restraints/parameters	24931/373/1118
Goodness-of-fit on F^2	1.010
Final R indexes [I>=2σ (I)]	R_1 = 0.0695, wR_2 = 0.1863
Final R indexes [all data]	R_1 = 0.1120, wR_2 = 0.2116
Largest diff. peak/hole/eÅ^{-3}	1.16/-1.11

$R_1 = \sum ||F_o|-|F_c|| / \sum |F_o|$. $wR_2 = [\sum w(F_o^2-F_c^2)^2 / \sum w(F_o^2)^2]^{1/2}$

Table S3. Bond lengths for **Ag_{17}**.

Bond	Length/Å	Bond	Length/Å
Ag1-Ag2	2.8461(15)	Ag4-S1	2.677(8)
Ag1-Ag3	3.3109(14)	Ag4-S1^4	2.614(5)
Ag2-Ag2^1	2.798(2)	Ag4-S2	2.576(5)
Ag3-Ag4	3.320(7)	Ag5-S1	2.26(3)
Ag3-Ag5	2.97(3)	Ag5-S1^4	2.89(3)
Ag1-S2	2.608(4)	Ag5-S2	2.84(4)
Ag2-S1	2.541(4)	Ag4-P1	2.445(11)
Ag3-S1	2.927(3)	Ag5-P2	2.35(4)
Ag3-S2^1	2.551(4)		

Table S4. Bond lengths for **Ag_{32}**.

Bond	Length/Å	Bond	Length/Å
Ag1-Ag2	2.810(2)	Ag9-Ag11	3.134(2)
Ag1-Ag6	2.998(2)	Ag10-Ag10[1]	3.287(3)
Ag1-Ag6[1]	2.912(2)	Ag1-S5	2.563(5)
Ag1-Ag7	2.7769(16)	Ag1-S6	2.521(5)
Ag1-Ag9	2.981(2)	Ag2-S1	2.646(5)
Ag1-Ag10	2.919(2)	Ag2-S2	2.704(5)
Ag1-Ag10[1]	2.913(2)	Ag3-S2	2.560(5)
Ag2-Ag3	2.979(2)	Ag3-S3	2.513(5)
Ag2-Ag3[1]	2.903(2)	Ag5-S3[1]	2.648(5)
Ag2-Ag4	2.7688(14)	Ag6-S4	2.659(5)
Ag2-Ag5	2.940(2)	Ag6-S5	2.678(5)
Ag2-Ag6	3.380(2)	Ag8-S1[2]	2.588(5)
Ag2-Ag6[1]	3.001(2)	Ag8-S3	2.668(5)
Ag3-Ag4	2.7663(15)	Ag8-S4	2.622(5)
Ag3-Ag5	2.916(2)	Ag9-S5	2.676(5)
Ag3-Ag5[2]	2.904(2)	Ag10-S6[2]	2.635(5)
Ag3-Ag6	2.806(2)	Ag11-S1	2.595(5)
Ag3-Ag12	2.934(2)	Ag11-S4[1]	2.611(5)
Ag4-Ag5	3.011(2)	Ag11-S6	2.680(5)
Ag4-Ag7	2.606(3)	Ag12-S2	2.600(5)
Ag5-Ag5[1]	3.277(3)	Ag5-Cl1	2.606(7)
Ag6-Ag7	2.7847(15)	Ag10-Cl4	2.589(6)
Ag6-Ag10	2.943(2)	Ag8-P2	2.405(5)
Ag7-Ag10	3.007(2)	Ag11-P1	2.393(5)
Ag8-Ag12	3.227(2)		

Reference

1. CrysAlis^{Pro} Version 1.171.36.31 (2012). Agilent Technologies Inc. Santa Clara, CA, USA.
2. G. M. Sheldrick, *Acta Cryst. A,* 2008, **64**, 112-122.
3. O. V. Dolomanov, L. J. Bourhis, R. J. Gildea, J. A.-K. Howard and H. Puschmann, *J. Appl. Cryst.* 2009, **42**, 339-341.
4. G. M. Sheldrick, *Acta Cryst. C*, 2015, **71**, 3-8.
5. C. Bannwarth, E. Caldeweyher, S. Ehlert, A. Hansen, P. Pracht, J. Seibert, S. Spicher and S. Grimme, *WIREs Comput. Mol. Sci.*, 2020, **11**.
6. C. Bannwarth, S. Ehlert and S. Grimme, *J. Chem. Theory Comput.*, 2019, **15**, 1652-1671.
7. S. Grimme, C. Bannwarth and P. Shushkov, *J. Chem. Theory Comput.*, 2017, **13**, 1989-2009.
8. S. Grimme, *J. Chem. Phys.*, 2013, **138**, 244104.
9. S. Grimme and C. Bannwarth, *J. Chem. Phys.*, 2016, **145**, 054103.